Dynamic Community Detection for Brain Functional Networks During Music Listening With Block Component Analysis

Yongjie Zhu, Jia Liu, and Fengyu Cong, *Senior Member, IEEE*

***Abstract*— The human brain can be described as a complex network of functional connections between distinct regions, referred to as the brain functional network. Recent studies show that the functional network is a dynamic process and its community structure evolves with time during continuous task performance. Consequently, it is important for the understanding of the human brain to develop dynamic community detection techniques for such time-varying functional networks. Here, we propose a temporal clustering framework based on a set of network generative models and surprisingly it can be linked to Block Component Analysis to detect and track the latent community structure in dynamic functional networks. Specifically, the temporal dynamic networks are represented within a unified three-way tensor framework for simultaneously capturing multiple types of relationships between a set of entities. The multi-linear rank-$(L_r, L_r, 1)$ block term decomposition (BTD) is adopted to fit the network generative model to directly recover underlying community structures with the specific evolution of time from the temporal networks. We apply the proposed method to the study of the reorganization of the dynamic brain networks from electroencephalography (EEG) data recorded during free music listening. We derive several network structures (L_r communities in each component) with specific temporal patterns (described by BTD components) significantly modulated by musical features, involving subnetworks of frontoparietal, default mode, and sensorymotor networks. The results show that the brain functional network structures are dynamically reorganized and the derived community structures are temporally modulated by the music features. The proposed generative modeling approach can be an effective tool for describing community structures in brain networks that go beyond static methods and detecting the dynamic reconfiguration of modular connectivity elicited by continuously naturalistic tasks.**

***Index Terms*— Dynamic community detection, brain connectivity, module detection, generative model, EEG, tensor decomposition, block term decomposition.**

Manuscript received 4 March 2023; revised 4 May 2023; accepted 12 May 2023. Date of publication 18 May 2023; date of current version 26 May 2023. This work was supported in part by the National Natural Science Foundation of China under Grant 91748105, in part by the National Foundation in China under Grant JCKY2019110B009 and Grant 2020-JCJQ-JJ-252, and in part by the Fundamental Research Funds for the Central Universities in the Dalian University of Technology in China under Grant DUT20LAB303. *(Corresponding authors: Yongjie Zhu; Fengyu Cong.)*

This work involved human subjects or animals in its research. Approval of all ethical and experimental procedures and protocols was granted by the Ethics Committee of the University of Helsinki, and performed in line with the Declaration of Helsinki.

Yongjie Zhu is with the Department of Computer Science, University of Helsinki, 00560 Helsinki, Finland, and also with the Department of Neuroscience and Biomedical Engineering, Aalto University, 00076 Espoo, Finland (e-mail: yongjie.zhu@helsinki.fi).

Jia Liu is with the Department of Biomedical Engineering, Faculty of Engineering, Lund University, 22363 Lund, Sweden (e-mail: jia.liu@bme.lth.se).

Fengyu Cong is with the School of Biomedical Engineering, Faculty of Medicine, and the School of Artificial Intelligence, Faculty of Electronic Information and Electrical Engineering, Dalian University of Technology, Dalian 116024, China, and also with the Faculty of Information Technology, University of Jyväskylä, 40014 Jyväskylä, Finland (e-mail: cong@dlut.edu.cn).

Digital Object Identifier 10.1109/TNSRE.2023.3277509

I. Introduction

THE functional architecture of the human brain can be characterized as a neuronal-synchronized network of interconnected brain regions [1], [2]. Many studies of electrophysiological brain networks have provided new insights into human behavior and cognition [3], [4], [5]. Early research focused on static functional connectivity (FC) patterns over time based on the stationary assumption. Recently, growing evidence has shown temporal dynamics of FC networks over multiple time scales during continuous task performance and resting states [6], [7], [8]. These network dynamics are critical to brain functions [9], [10] and dysfunctions [11], [12], [13]. Although brain networks dynamically fluctuate over time, FC networks tend to be temporally clustered into a finite number of putative connectivity states, that is, distinct connectivity modules (communities or subnetworks) that transiently form and dissolve during continuous task performance [14], [15], [16]. Most of the research on dynamic FC states concentrates on the transition among whole-brain network profiles only considering connectivity edges [14], [17], [18]. However, few studies focus on temporally switching in the topological organization of functional brain networks such as the modular or community structure.

Evidence from network neuroscience studies demonstrates complex topological structures of both structural and functional brain networks [19], [20], where the brain networks can be decomposed into clusters of densely interconnected nodes (referred to as modules or communities) that are relatively

sparsely connected with nodes in other communities/modules. These topological communities typically correspond to clusters of anatomically neighboring and/or functionally related brain regions which are involved in specialized functional components [18], [20], [21]. Numerous community detection algorithms have been developed for identifying underlying community structures in brain networks. The most widely used method in neuroimaging analysis is to apply modularity maximization to the static brain networks, where nodes are partitioned into non-overlapping and densely inter-connected modules by maximizing an objective function of modularity [22]. Most of them are only suited for analysis of static or single-layer networks to define candidate communities at a fixed time [23], but characterizing time-evolving networks with community structures has received less attention.

The related studies for time-evolving networks primarily focus on identifying clusters of a set of snapshots, i.e. network connectivity patterns, that repeat themselves across time [14], [15]. For example, Ou and his colleagues introduced an approach based on statistical state modeling to identify the network states through hierarchical clustering followed by a Hidden Markov Model (HMM) [24]. In a similar manner, Ma et al. identified the network states and their transitions through independent vector analysis and Markov modeling [25]. Vidaurre and colleagues have recently developed multiple methods based on HMM and applied them to neuroimaging data, suggesting that functional networks transiently reorganize on the timescale of milliseconds [15], [16], [26], [27]. Under the subspace modeling approaches, principal component analysis (PCA) [28] and independent component analysis [29] are used to extract the FC patterns, where it is assumed that brain networks are composed of eigenconnectivities or independent components. An alternative popular approach is based on k-means clustering of dynamic functional connectivity networks (dFCNs) across time to identify the FC-states during rest, where it is assumed that a finite number of FC patterns recur across time [14]. Although these methods were beneficial to summarize the overall dynamic brain activity, they failed to uncover the topological properties of the whole-brain networks.

Although dynamic community detection technique [30] has recently emerged as a powerful tool for tracking the topological reconfiguration of brain networks [18], [31], [32], [33], it is still not straightforward for module detection for time-varying networks within or across multiple subjects. We thus consider the tensor decomposition (or tensor component analysis) based methods for such dynamic community detection [18], [31], [34], [35], [36], [37] since the tensor decomposition enables multi-timescale dimensionality reduction both within and across temporal evolution for multiple subjects in a purely data-driven method. Tensor decomposition has recently been regarded as an extension of PCA for dynamic brain network analysis across subjects, where time-frequency vectorized adjacency matrices were formed into a tensor and decomposed into components characterizing brain network patterns with spectral-temporal features [9], [38], [39], [40] or temporal features [41], [42]. However, in this case, the topological organization of brain networks is unable to be directly revealed in the resulting components. For such community detection in temporal brain networks, tensor-based approaches typically model a network as a three-way tensor and apply low-rank tensor decomposition to extract latent components [42], [43]. Each component is made up of three factors named "loading factors". Two of the factors relate to nodes and are used to generate a community with clustering or binary classification [43]. The other loading factor contains temporal information for tracking the temporal evolution [42]. Despite that these tensor-based methods have achieved success in dynamic community detection for brain network analysis, further analysis, such as k-means clustering or classification of node loading factors, is required after tensor decomposition to generate the community [34], [36]. Additionally, these approaches with tensor decomposition fail to provide a good generative model for the dynamic brain networks; more precisely, the physical interpretations of the factors related to nodes and the temporal dimension are unclear.

In this paper, to overcome the limitations mentioned above, we introduce a framework based on a latent network generative model and block term decomposition (BTD) [44], a variant of tensor decomposition [45], [46], [47], for detecting dynamic community evolution in time-varying brain networks during music listening. We first formulate a generative model to characterize community structure in time-varying brain networks, quantified by envelope correlation of EEG recorded during free music listening. Then, we show how to link the generative model to BTD and use it to learn the latent community structures. Specifically, temporal concatenated connectivity matrices are organized into a three-way tensor. Then, BTD with rank-$(L_r, L_r, 1)$ term is applied to extract the underlying community structures with a specific temporal mode. Different from previous tensor decomposition such as CANDECOMP/PARAFAC (CP) model for brain network analysis, the factors with rank L_r are able to characterize L_r communities after the multi-linear rank-$(L_r, L_r, 1)$ BTD, which can discover the topological structures of brain networks. Actually, the CP model can be considered as rank-$(1, 1, 1)$ decomposition and it is unable to reveal the community structures so further analysis is needed for the loading factors related to the node. After BTD, time series of five long-term acoustic features were extracted from the audio stimuli by music information retrieval techniques used in previous studies [9], [48]. Finally, we analyzed the correlation between temporal factors and the musical feature time series to identify underlying community structures of brain networks modulated by musical features.

The main contributions of this work are three-fold. First, we propose a generative model to characterize the temporal community evolution for dynamic brain functional networks. Second, we show the proposed generative model can be fitted with multilinear rank-$(L_r, L_r, 1)$ BTD to learn the latent community structures in the time-varying brain networks without further analysis of the resulting BTD components. Third, the proposed framework is then used for EEG networks during naturalistic music listening to identify music-modulated

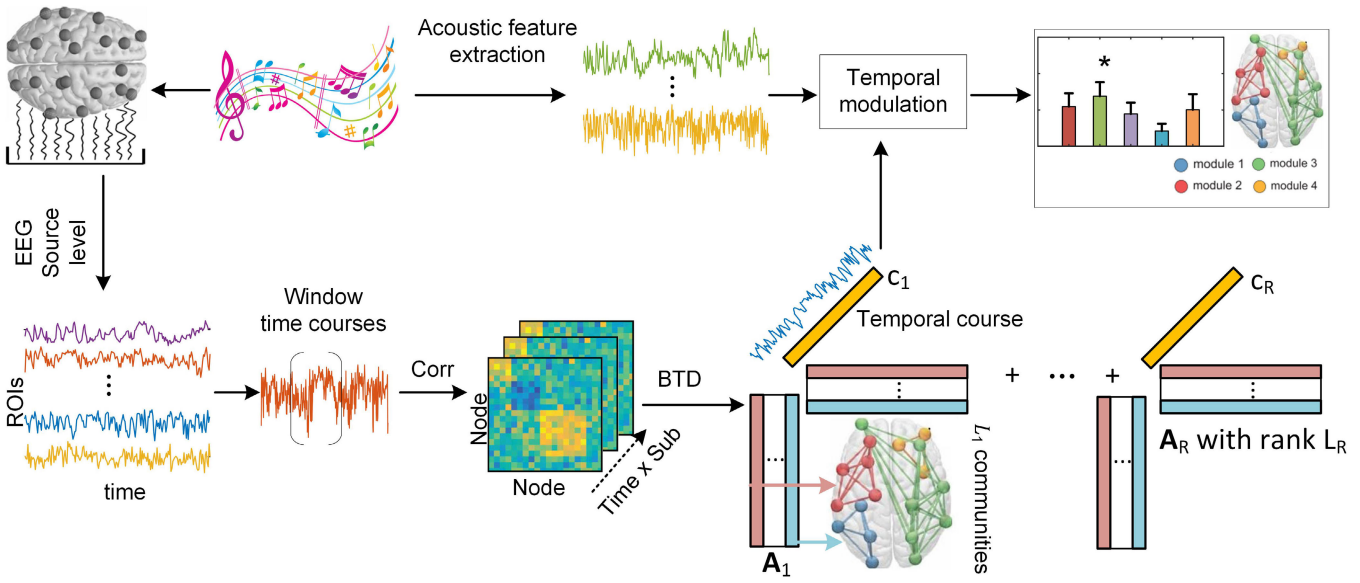

Fig. 1. **Analysis pipeline.** EEG data were recorded during continuous music listening and then source-localized with wMNE. Source-localized data were parcellated into 68 ROIs based on an anatomical brain template. After signal leakage correction, the Hilbert transformation was applied to extract the amplitude envelopes of the ROIs' time courses. An adjacent matrix was thus obtained by computing the correlation between the envelope of separate regions for each time window. Then a three-way tensor was formed including two node modes and a temporal mode. Nonnegative BTD decomposition was applied to the temporally concatenated tensor across subjects. The node factor matrix of extracted components with rank-L_r is able to characterize the topological structures of the latent network patterns, which encodes L_r communities or node clusters, and the temporal courses represent the time evolution of the modular patterns. On the other hand, musical features were extracted using acoustic feature extraction. The temporal courses of decomposed components and musical feature time series were analyzed to examine the modulated brain networks.

community structures, which demonstrate its effectiveness in time-varying modular detection for brain networks.

II. Materials and Methods

A. Notation

In this paper, scalars are denoted by lowercase letters $(a, b, \cdots)$, vectors are denoted by boldface lowercase letters, such as $(\mathbf{a}, \mathbf{b}, \cdots)$, matrices are written in boldface uppercase letters $(\mathbf{A}, \mathbf{B}, \cdots)$, and high order tensors by boldface calligraphic letters $(\mathcal{A}, \mathcal{B}, \cdots)$. Operator $\circ$ represents outer product of vectors, $\otimes$ denotes the partitionwise Kronecker product, $\odot$ represents Khatri–Rao product and $\odot_c$ denotes columnwise Khatri–Rao product [49]. The superscripts $\cdot^T$ and $\cdot^\dagger$ indicate the transpose and Moore–Penrose pseudoinverse, respectively.

B. Data Description and Preprocessing

EEG data from 14 right-handed adults between the ages of 20 and 46 were used in the current study. No participant reported a history of hearing loss or neurological disease and none of them had music expertise. This research was approved by the local ethics committee and has no conflicts of interest. We presented subjects with a piece of music, which was played via audio headphones. The used music was a 512-second long musical segment of modern tango, which had a suitable duration for the experimental setting due to its high range of fluctuation in several musical features [9], [50]. EEG data were collected at a sampling rate of 2048 Hz with BioSemi electrode caps of 64 channels when participants were naturally listening to the continuous musical segment.

In this paper, we studied five well-known long-term acoustic features consisting of tonal and rhythmic features, which were computed by using a frame-by-frame analysis technique [48], [50]. we set the length of each frame as three seconds and the overlap between adjacent frames as two seconds. Thus, a time course with 510 samples was created for each musical feature with a sampling rate of 1 Hz. The five acoustic features include two tonal musical features, Mode and Key Clarity, and three rhythmic features, consisting of Fluctuation Centroid, Fluctuation Entropy, and Pulse Clarity.

In preprocessing steps, EEG data were re-referenced by common average electrodes and were visually inspected to reject typical artifacts. We interpolated bad channels with a mean value of their spherical adjacent channels. We used a 50 Hz notch filter to remove powerline interference. High-pass and low-pass filters with 2 Hz and 35 Hz cutoffs were then applied since our previous investigation of the frequency range revealed that no useful information was observed in higher frequencies [48], [51]. Finally, we down-sampled the EEG data to 256 Hz. Independent component analysis (ICA) was applied to individual EEG data to remove EOG artifacts (e.g. eye blinks) [52].

The schematic diagram of subsequent data processing is shown in Figure 1. Following data preprocessing, we estimated the forward model and inverse model using a MATLAB-based toolbox Brainstorm [53]. The symmetric boundary element method (BEM) was applied to compute the forward model with a default MNI MRI template (Colin 27). To solve the inverse model, we used weighted minimum-norm estimate (wMNE) [54]. The reconstructed cortical surface was decimated to 4098 evenly distributed vertices per hemisphere with 4.9 mm spacing. Depth-weighted L2-minimum-norm estimate was computed for all current dipoles with a loose

orientation of 0.2. The inverse solution was noise-normalized. Then, the cortical surface was parcellated into 68 anatomical regions based on the Desikan-Killiany Atlas (DKA) [55]. For each parcel, we performed a principal component analysis to extract orthogonal components that describe the activity, ordered by amount of variance explained. We selected the first principal component as a representation of the parcel's time course of activity. Thus, for each subject, a source-level data matrix $\mathbf{P}$ was created with dimension $n \times n_t$, where $n = 68$ represents the number of anatomical regions and n_t represents the number of samples.

C. Dynamic Functional Connectivity Network Construction

We attempt to obtain an all-to-all whole-brain FC network by computing connectivity between all pairs of DKA regions. In M/EEG, a significant confound of electroencephalography source connectivity is that the ill-posed inverse problem and inaccuracies in the forward solution lead to a degree of spatial ambiguity and mislocalization of source [29], [56]. In other words, two source-level time signals (e.g. from two brain regions) might be significantly correlated, merely due to 'signal leakage' [17]. The obtained connectivity between spatially separate brain areas might be inaccurate without careful control. To solve this issue, we performed the orthogonalization of source-reconstructed signals, a widely used technique for leakage reduction [29]. Following signal leakage correction, the Hilbert transformation was applied to extract the amplitude envelopes of the time courses. The dynamic FC networks were constructed for each subject by calculating the Pearson correlation, $\boldsymbol{X} \in \mathbb{R}^{n\times n}$, between different $n = 68$ DKA regions using a sliding window approach [14]. The rectangular window length was set as 3 seconds and the overlap was 2 seconds between two adjacent windows, resulting in a sampling rate of 1 Hz in the temporal dimension. This sampling rate was in line with the musical feature time series.

For each subject, a sequence of functional brain networks $\mathcal{G} = \{G_t(V, E_t)|t = 1, \ldots, \tau_w\}$ is constructed, where G_t is the network snapshot at time t, $V = \{v_i\}_{i=1}^{n}$ is a set of n nodes and E_t is the set of edges at time step t. Here, the nodes are the 68 DKA regions ($n = 68$), and the edges E_t are constructed with $\boldsymbol{X}_t$, which is the adjacency matrix representing the network at time step t. $\tau_w = 510$ is the total number of time windows. The adjacency matrices were temporally concatenated across subjects, resulting in a group-level functional brain network $\mathcal{G}$ with $\tau = \tau_w \times n_p$, where n_p is the number of subjects.

D. Generative Model for Dynamic Functional Networks

To allow module detection, we here extend the temporal clustering model under the CP framework in [34] to a generative model under the BTD framework. We model a dynamic network functional brain networks $\mathcal{G} = \{G_t(V, E_t)|t = 1, \ldots, \tau\}$ as a mixture of R generative models$\{S^r\}_{r=1}^{R}$. S^r contains the same set of nodes V, for $r = 1, \ldots, R$, with L_r communities (or subnetworks/modules) $\{C_{l_r}^r\}_{l_r=1}^{L_r}$. We assume that the probability that a node $i \in V$ belongs to a community $C_{l_r}^r$ in S^r follows a Bernoulli distribution, denoted as $P(i \in C_{l_r}^r) = a_{il_r}^r$. At time step t, the l^{th} community in the r^{th} generative model S^r generates the connection between two nodes i, j with probability $a_{il_r}^r a_{jl_r}^r \lambda_t^r$, where λ_t^r is defined as an connection-generating rate or strength. λ_t^r changes throughout time and can be modeled as a time series, which here represents the temporal evolution of the communities. Consequently, the r^{th} generative model S^r generates the edge with the sum across L_r communities at time step t:

$$(a_{il_1}^r a_{jl_1}^r + \cdots + a_{il_r}^r a_{jl_r}^r + \cdots + a_{iL_r}^r a_{jL_r}^r)\lambda_t^r = \sum_{l_r=1}^{L_r} (a_{il_r}^r a_{jl_r}^r)\lambda_t^r \tag{1}$$

which could be considered as the expected number of connections generated between i and j in S^r at time t.

Align and compact adjacency matrices, $\boldsymbol{X}_t$, temporally into the third mode of a third-order tensor, namely $\boldsymbol{\mathcal{X}}_{::t} = \boldsymbol{X}_t$, $t = 1, \ldots, \tau$. Element $\mathcal{X}_{ijt}$ can be interpreted as the number of connections (the strength of connections) observed between node i and j at time step t. Thus, the model approximates $\mathcal{X}_{ijt}$ by summing the Eq. (1) across R generative models as follow:

$$\mathcal{X}_{ijt} \approx \sum_{r=1}^{R} \left(\sum_{l_r=1}^{L_r} (a_{il_r}^r a_{jl_r}^r)\lambda_t^r\right) \tag{2}$$

In other words, the dynamic community detection problem is here to find R network generative models S^r (or latent source components), their temporal evolution (connection-generating) λ_t^r, and the probability that node i belongs to the one of communities in the generative source S^r, $a_{il_r}^r$, for $r = 1, \ldots, R$; $t = 1, \ldots, \tau$; $l_r = 1, \ldots, L_r$; and $i = 1, \ldots, n$. We can thus formulate the objective function as follow:

$$\begin{aligned} \min \sum_{i,j\in V} \sum_{t} \|\mathcal{X}_{ijt} - \sum_{r=1}^{R} \left(\sum_{l_r=1}^{L_r} (a_{il_r}^r a_{jl_r}^r)\lambda_t^r\right)\|_F^2 \\ \text{s.t. } 0 \le a_{il_r}^r \le 1; \quad \text{for } i = 1, \ldots, n \\ \lambda_t^r \ge 0 \end{aligned} \tag{3}$$

We suppose that the number of the generative components R and the community number L_r, $r = 1, \ldots, R$ in each component are given here merely for simplicity of exposition.

E. Learning Dynamic Community Structures With Rank-(L, L, 1) BTD Model

To estimate the community structure in Eq. (3), we rewrite $\sum_{r=1}^{R}(\sum_{l_r=1}^{L_r}(a_{il_r}^r a_{jl_r}^r)\lambda_t^r)$ in Eq. (3) to $\sum_{r=1}^{R}(\boldsymbol{a}_i^r \boldsymbol{a}_j^{rT} \lambda_t^r)$ with vector format, where $\boldsymbol{a}_i^r \in \mathbb{R}^{L_r}$. The optimization problem in Eq. (3) can further be rewritten as,

$$\begin{aligned} \min_{\mathbf{A}_r, \mathbf{c}_r} \|\boldsymbol{\mathcal{X}} - \sum_{r=1}^{R} (\boldsymbol{A}_r \cdot \boldsymbol{A}_r^T) \circ \boldsymbol{c}_r\|_F^2 \\ \text{s.t. } 0 \le \mathbf{A}_r \le 1; \quad \text{for } r = 1, \ldots, R \\ \mathbf{c}_r \ge 0 \end{aligned} \tag{4}$$

where $\mathbf{A}_r := [\boldsymbol{a}_1^r \cdots \boldsymbol{a}_n^r] \in \mathbb{R}^{n\times L_r}$, $\mathbf{c}_r := [\lambda_1^r \cdots \lambda_\tau^r]^T \in \mathbb{R}^{\tau}$. Surprisingly, the optimization problem in Eq. (4) can be solved

Algorithm 1 ALS

Input: ALS($\boldsymbol{\mathcal{X}} \in \mathbb{R}^{n\times n\times \tau}$, R, $L_1, L_2, \ldots, L_R$)
Output: $\mathbf{A} \in \mathbb{R}^{n\times \hat{R}}$, $\mathbf{C} \in \mathbb{R}^{\tau\times \hat{R}}$

```
begin
    initiazation for A, C
    repeat
        Update A:
        Ã = [(A ⊙ C)† · (A ⊙ C) · A^T]_+^T
        for r = 1 to R do
            Ã_r = QR QR-factorization
            A_r ← Q
        end
        A = [A_1 ··· A_R]
        Update C:
        T = (A_1 ⊙_c A_1)1_{L_1} ··· (A_R ⊙_c A_R)1_{L_R}
        C ← [T† · T · C^T]_+^T
    until convergence;
end;
```

by using the BTD framework with rank-$(L_r, L_r, 1)$ [44]. The multilinear rank-$(L_r, L_r, 1)$ terms decomposition factorizes a three-way tensor into a sum of R low multilinear rank terms, each of which can be written as the outer product of a rank L_r matrix and a vector as shown in Eq. (4). Loading matrix $\mathbf{A}_r$ with rank-L_r is able to characterize the modular structures of the latent network pattern, which encodes L_r communities or node clusters since the elements represent the probability that the n nodes belong to which communities. The node cluster of each community can be obtained by the largest entry in the corresponding row of $\mathbf{A}_r$. That is, if $k = \arg\max_j\{(\mathbf{A}_r)_{ij}\}$, then node v_i belongs to k^{th} node cluster. $\mathbf{c}_r$ characterizes the temporal evolution of the community structures (see Fig. 1).

Like CP-based tensor decomposition, there are many approximate algorithms for rank-$(L_r, L_r, 1)$ BTD decomposition, such as multiplicative updating (MU) method, alternating least squares (ALS) and hierarchical alternating least squares (HALS) [57]. Here, we use the structured data fusion ALS implementation by the Tensorlab [58], which is so far the most widely used computation scheme for the BTD model. The ALS algorithm applies a gradient descent method to solve the minimization problem in Eq. (4) iteratively. At each iteration, one of the factor matrices is updated while other factor matrices are fixed. We define $\mathbf{A} := [\mathbf{A}_1 \cdots \mathbf{A}_R] \in \mathbb{R}^{n\times \hat{R}}$, $\mathbf{C} := [\mathbf{c}_1 \cdots \mathbf{c}_R] \in \mathbb{R}^{\tau\times \hat{R}}$, where $\hat{R} = \sum_{r=1}^{R} L_r$. For brief illustration, consider estimating $\mathbf{A}$, fixing $\mathbf{C}$, resulting in the following update rule:

$$\mathbf{A} \leftarrow \arg\min_{0\le \mathbf{A}\le 1} \|\mathrm{X} - \sum_{r=1}^{R} (\boldsymbol{A}_r \cdot \boldsymbol{A}_r^T) \circ \boldsymbol{c}_r\|_F^2, \quad \text{for fixed } \mathbf{C} \tag{5}$$

It can be estimated as a linear least-squares problem and has a closed-form solution. The update procedure for $\mathbf{A}$ and $\mathbf{C}$ is summarized in Algorithm 1. The detailed solution of rank-$(L_r, L_r, 1)$ terms decomposition using ALS and its convergence analysis can be found in [44] and [49].

F. Model Order Selection

When estimating the multi-linear rank-$(L_r, L_r, 1)$ BTD model, a natural question follows: how to select R and L_r from the experimental data? So far there is unfortunately still no gold standard method for model order selection of the BTD model in the literature [59]. A common practice is to determine R and L_r that result in rational decomposition results according to the data fitting values and the prior knowledge of data features. Here, we use the model fitting method, based on the measurement of the data fitting, as a reference to choose the model order. Data fitting is computed based on model reconstruction error and the explained variance of data. Let component number $R \in [1, \mathcal{R}]$ and the rank $L_r \in [1, \mathcal{L}]$, where $\mathcal{R}$ and $\mathcal{L}$ are the empirically maximal number of latent components and rank. The data fit can be obtained as

$$Fit(R, L_r) = 1 - \frac{\|\boldsymbol{\mathcal{X}} - \sum_{r=1}^{R} (\boldsymbol{A}_r \cdot \boldsymbol{A}_r^T) \circ \boldsymbol{c}_r\|_F^2}{\|\boldsymbol{\mathcal{X}}\|_F^2} \tag{6}$$

We can fix one of them, R or L_r to examine the changes in the data fitting. Unlike PCA, the estimation of BTD may have local minima (suboptimal solution), and not guarantee that optimization routines will converge to the global optimal solution. Thus, we run the ALS optimization procedure at each component number R or each rank value L_r 20 times from random initial conditions. Generally, the candidate model order $\widetilde{R}$ and rank $\widetilde{L_r}$ can be thought of as the appropriate selection when the data fitting no longer increases as the number increases.

G. Temporal Modulation of the Community Structure by Musical Features

To examine how musical features temporally modulate the topological (module) structures of brain functional networks, we here adopt temporal modulation analysis for each musical feature, time courses of modular structures (components), and subject. Previous studies have shown that the topological organization of functional networks temporally evolves to support ongoing cognitive function [14], [29]. We here attempt to perform a correlation analysis between the temporal courses of modular patterns and musical time series, by assessing the statistical significance of temporal correlations based on a surrogate permutation procedure [9], [29]. We obtain R BTD components with two loading factors, characterizing the temporal evolution (represented by $\mathbf{c}_r$) and topological structures of brain networks (represented by $\mathbf{A}_r$ with rank L_r). The temporal factor matrix $\mathbf{C}$ ($\mathbf{C} \in \mathbb{R}^{\tau\times \hat{R}}$) is first reshaped as a three-way tensor $\boldsymbol{\mathcal{C}}$ ($\boldsymbol{\mathcal{C}} \in \mathbb{R}^{\tau_w\times n_p\times R}$). which consists of an individual time course for each BTD component. For each BTD component and each subject, we calculate the correlation coefficients between each musical feature time series and time courses as the modulation scores. We then evaluate which BTD component is significantly modulated by examining whether its modulation score is significantly different from the scores

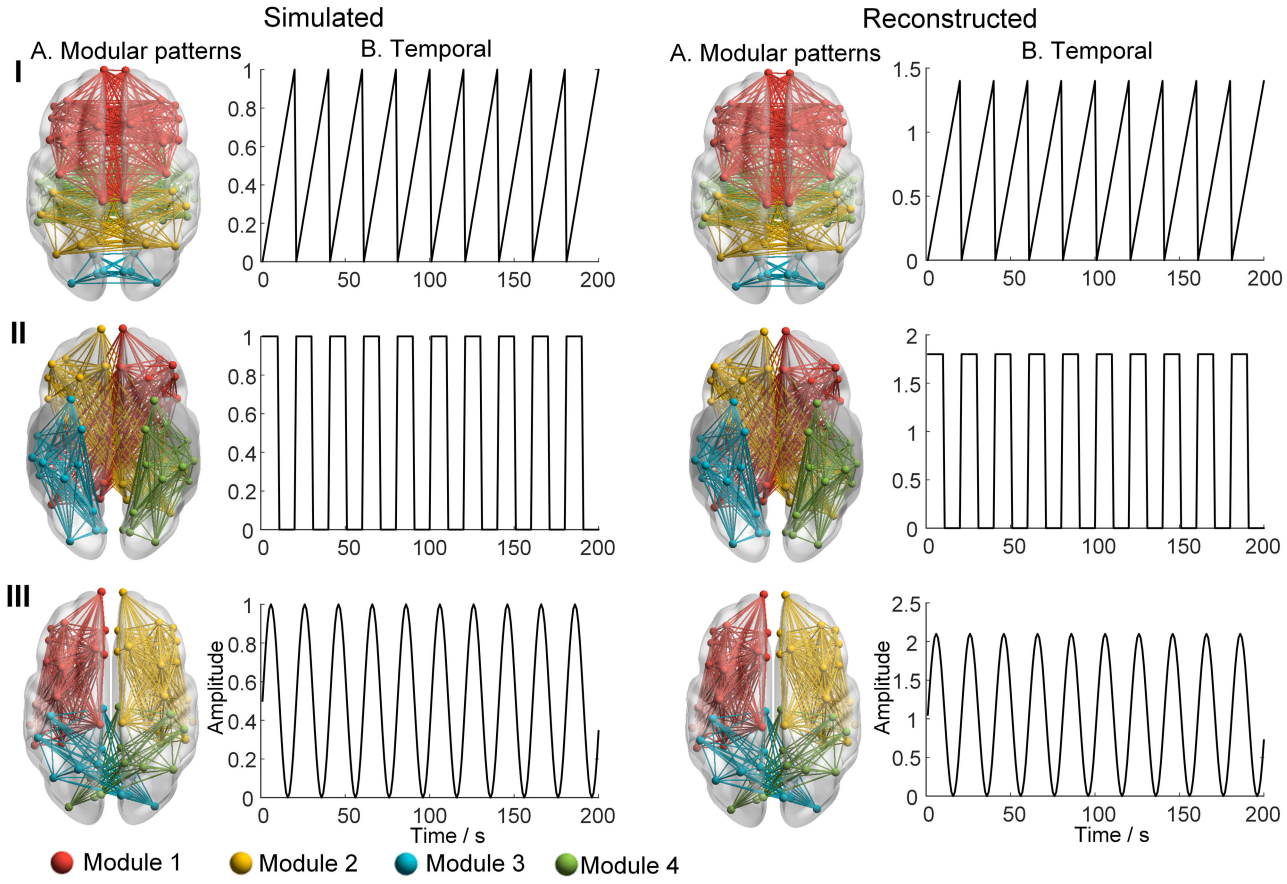

Fig. 2. **Results of simulation data.** Left: the modular structures and temporal profiles of three synthetic brain network patterns. Right: the corresponding modular structures and temporal profiles of reconstructed brain patterns. I, II, and III represent the three components respectively. Note that the scale of the amplitude is different between simulated and reconstructed temporal profiles due to the scaling indeterminacy in tensor decomposition.

of surrogate data. We generate the surrogate data with a phase-randomization procedure [60], which randomizes the intrinsic phase and retains the properties of the temporal course in the spectral domain. The phase-randomization procedure is repeated 5000 times for each BTD component. We compute the correlation coefficients between musical feature time series and phase-randomized time courses to generate a distribution of modulation scores from surrogate data. The 95^{th} percentile ($p = 0.05$) of surrogate modulation scores are chosen as the threshold (the control modulation score for comparisons) for each subject. This significant level was corrected based on Bonferroni correction for multiple comparisons across the multiple components i.e., $p_{correct} = 0.05/R$. For each component, we finally use two-tailed t-tests for the modulation score of each musical feature to determine which component (brain network pattern) is modulated significantly differently at $p_{correct} = 0.05/R$ level from the defined threshold.

III. Results

A. Simulation Results

We first validated the proposed approach with simulation data, which provided the instruction to study the performance of the methodology. The performance of the Pearson correlation of the envelope with signal leakage reduction, as a metric to investigate functional connectivity at the source level, has been well validated in a previous study [29]. Therefore, we would not test the performance of connectivity metrics repeatedly in the current study. We only validated the ability of rank-$(L_r, L_r, 1)$ BTD, for dynamic functional networks, to extract the community structures and the temporal evolving over time scales of minutes.

We constructed dynamic functional networks with adjacency matrices ($n = 68$ nodes, $\tau = 200$ time points). The tensor representation of the networks was obtained by the outer product of adjacency matrices and temporal profiles. That is, $\boldsymbol{\mathcal{M}}_{sim} = \boldsymbol{\mathcal{S}}_{sim} + \boldsymbol{\mathcal{N}}_{sim} = \sum_{r=1}^{R} (\boldsymbol{A}^r_{sim} \boldsymbol{A}^{r\ T}_{sim}) \circ \boldsymbol{c}^r_{sim} + \boldsymbol{\mathcal{N}}_{sim}$, where $\boldsymbol{\mathcal{N}}_{sim} \in \mathbb{R}^{n \times n \times \tau}$ is a noise tensor with dimensions same as $\boldsymbol{\mathcal{S}}_{sim}$. We predefined three community structures ($R = 3$) and each of them included four communities or node clusters ($L_r = 4, r = 1, 2, 3$). We generated binary networks by using the node clusters. Their temporal evolution was modulated by triangle, square, and sine waves (Fig. 2). We showed the case under the signal-to-noise ratio (SNR) of 10dB. One can observe that the three latent brain network patterns with distinct topological structures and temporal modes were successfully extracted using multilinear rank-$(L_r, L_r, 1)$ BTD.

B. Results From EEG Data Recorded During Music Listening

The proposed method was applied to dynamic functional networks constructed from the naturalistic music listening

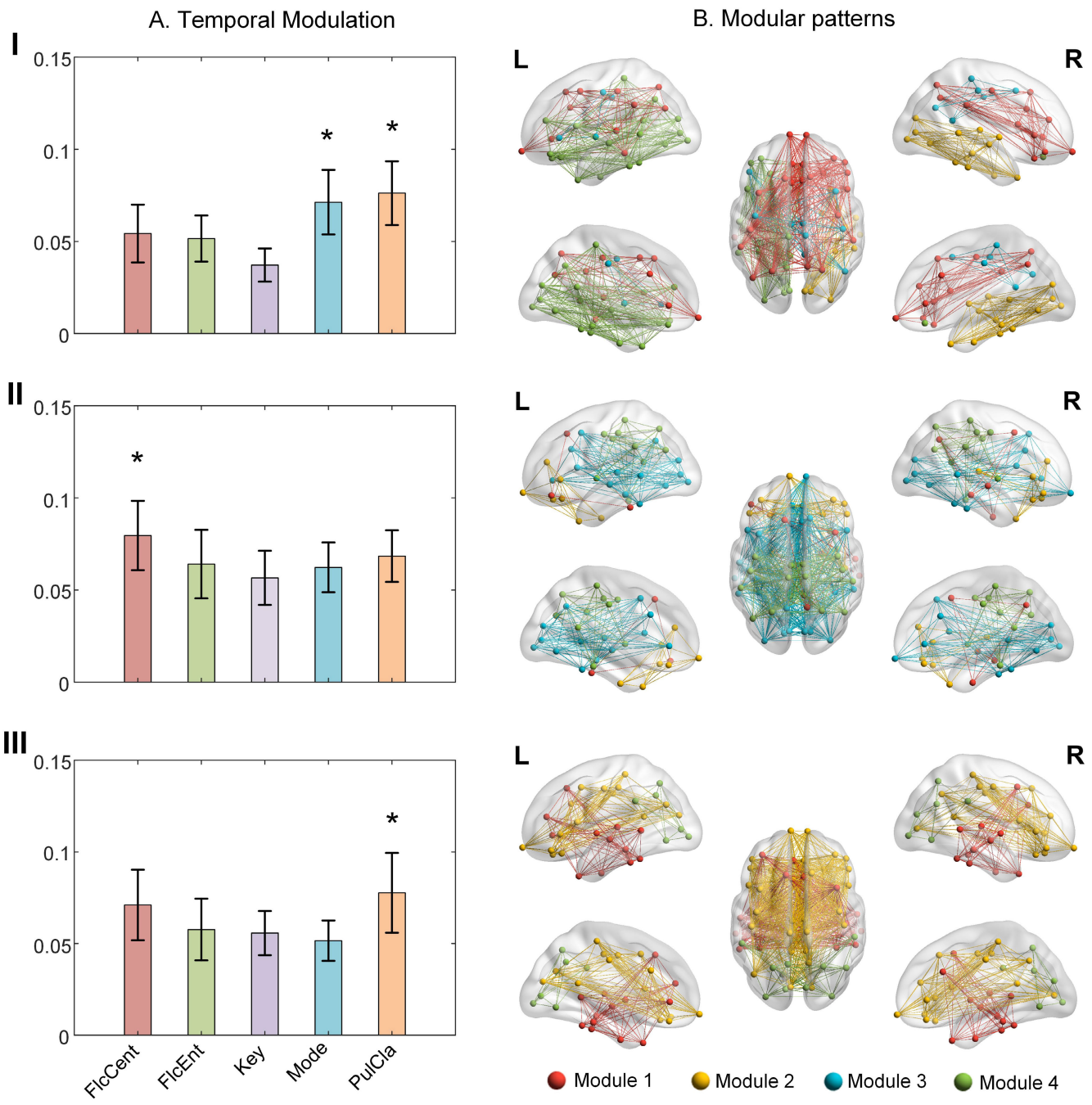

Fig. 3. **Results from music-listening data.** A. For each subject, the modulation scores are estimated from the correlation analysis of temporal courses of BTD components and music features (see Section II-G). Error bars display the standard errors of the mean across subjects. An asterisk shows that the BTD component is modulated significantly differently ($p < 0.05$; corrected) from the surrogate data. B. The modular patterns of 3D visualization. Each dot/node indicates one brain region of the DKA atlas and nodes in the same community have the same color. The node cluster or community is obtained from the $\mathbf{A}_r$ matrix with rank L_r, which encodes the node membership information. Row I shows two unilateral auditory modules, sensorimotor and frontoparietal modules; row II indicates strong frontotemporal and temporoparietal modules; row III shows frontotemporal and frontoparietal subnetworks.

EEG dataset to detect the community structures across subjects. Fig. 3 shows the estimated brain network with specific modular patterns from BTD components: their modular structure profiles and their modulation scores by five musical features. The mean and standard deviation of the modulation score were reported across subjects. Here, $R = 5$ components (with 4 community clusters for each, that is, $L_r = 4, r = 1, \ldots, R$) were extracted by BTD based on data fitting analysis (see Fig. 4), and we presented 3 components that showed significant musical feature modulation. We observed unilateral auditory modular subnetworks (modules 2 and 4 in Row I of Fig. 3) and two bilateral frontoparietal functional subnetworks (modules 1 and 3 in Row I of Fig. 3). The auditory subnetworks showed strong clustering in the temporal lobe. The regions involved by the frontoparietal subnetworks were part of the frontoparietal network (FPN), which here was composed

of the dorsolateral prefrontal cortex and posterior parietal cortex. Such community structures were temporally modulated by the Mode and Pulse Clarity features. Row II of Fig. 3 showed the sensorimotor networks (module 4), frontotemporal subnetworks (modules 1 and 2), and temporoparietal subnetworks (module 3), which seemed to be related to the anterior higher-order cognitive brain networks in accordance with previous literature [27]. The involved regions were part of the default mode network (DMN) which here contains temporal poles, the ventromedial prefrontal cortex, and the posterior cingulate cortex. They also involved Broca's area which was often associated with semantic integration. The time course of this modular pattern was significantly modulated by the Fluctuation Centroid. There were three modules detected in Row III, showing strong clusters in the visual subnetworks, frontotemporal and frontoparietal subnetworks. This modular pattern was significantly modulated by the Pulse Clarity.

IV. Discussion

In this study, we proposed a BTD-based framework applied to EEG data, which enabled us to characterize the dynamic topological properties of electrophysiology brain networks during natural music listening. We formed a three-way tensor including temporal evolution of functional connectivity at the source level and then applied multilinear rank-$(L_r, L_r, 1)$ decomposition to detect the modular structures of time-varying brain networks. We derived large-scale brain network topological structures during freely listening to music, which was characterized by BTD components. Such BTD component, we referred to as a modular pattern, was represented with a distinct topological pattern of functional networks across the set of predefined atlas regions spanning the whole brain. These modular patterns of topology-specific envelop-coupling were found to be temporally modulated by musical features and corresponded to plausible brain functional sub-systems, consisting of auditory, sensorimotor, and higher-order cognitive subnetworks. To the authors' knowledge, this might be the first complete formulation of a BTD-based generative model method for module detection of electrophysiology brain networks using ongoing EEG.

Simulation results showed the effectiveness of the proposed method for the detection of community structure in time-varying brain functional networks. When applied to the EEG data recorded during the continuous music listening task, the proposed approach identified more diverse community structures in addition to the typical assortative organization in brain networks, which was related to auditory and semantic information processing as well as higher-order cognitive functions. These types of network architecture seemed to be associated with music perception and were temporally modulated by the acoustic musical feature extracted from music. Their topological structures might allow the network to engage in a wider functional repertoire, e.g., integration of information across different brain regions in higher-order cognitive processes. Different from CANDECOMP/PARAFAC(CP)-based methods, our proposed method allowed the mutual existence of multiple communities (modules or subnetworks) in the same components (brain patterns) due to the multi-linear rank decomposition. For example, we found bilateral frontotemporal communities (modules 2 and 4 of Row II in Fig. 3) involved a subdivision of the DMN network that subserves a semantic integration and the ventromedial prefrontal cortex was typically specialized for emotion regulation. The subnetworks also involved Broca's areas, which are typically related to language processing. Previous studies demonstrated that brain functional networks engaged in music processing have strict similarities with that of language processing [61], [62]. Thus, the nodes of the subnetwork including Broca's areas could be implicated during continuously listening to music. These subnetworks were also identified in the previous study with two independent CP components based on CP-based methods [9].

We also observed bilateral frontoparietal communities (modules 1 and 3 of Row I in Fig. 3) in the FPN network that subserved an integrative function between periphery communities in the left and the right hemisphere during auditory or semantic comprehension and unilateral auditory subnetworks (modules 1 and 3 of Row I). This asymmetry modules 2 and 4 might be associated with the language network that displays some degree of hemispheric lateralization. The nodes of the language network would be implicated during naturalistic language comprehension task performance. Indeed, this left lateralized subnetwork is anchored in the angular gyrus with extensions to the inferior frontal gyrus, inferior temporal gyrus, and a number of nodes spanning the inferior to superior precentral gyrus. These regions are consistent with previous accounts of semantic cognition [61], [62]. The parietal module (module 4 of Row II in Fig. 3) was related to the motor networks and it was believed that perception and execution of actions are strongly coupled in the brain as a result of learning a sensorimotor task, which facilitated not only predicting the action of others but also interacting with them [63]. During music listening, a tight coupling emerged between the perception and production of sequential information in hierarchical organization [9], [63]. Brain regions associated with motor networks could be involved due to imitation and synchronization during musical activities (e.g. ensemble playing or singing). These subnetworks involved in auditory areas (Row III in Fig. 3) played an important function in music perception in agreement with previous studies [9], [50].

Tensor decomposition especially with CP model analysis methods has been applied for the multi-way neuroimaging data in cognitive research since it enables multi-timescale dimensionality reduction both within and across subjects or conditions with unsupervised learning [9], [39], [48]. This provides the possibility of module detection of dynamic time-varying brain functional networks. The majority of studies for brain networks typically applied the CP model to examine the temporal, spectral, or spatial features of brain connectivity networks, which is unable to detect the modular structure in resulting CP components simultaneously. This results in the requirement for further analysis such as clustering of the network factor of CP components when looking at the topological structure of the networks. To overcome this limitation, the proposed methods adopted block component analysis, rank-$(L_r, L_r, 1)$ BTD. The resulting BTD components include the

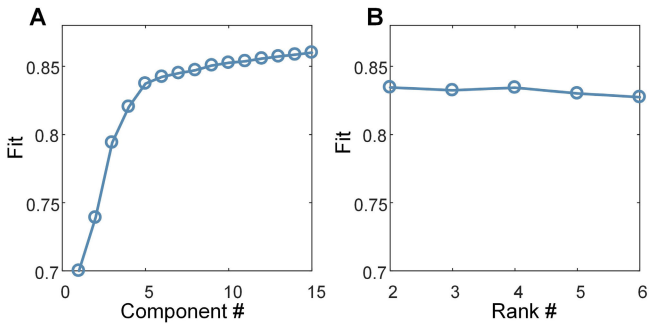

Fig. 4. **Data fitting curves in the function of the component number and rank number.** A. Fit versus component number R obtained by computing the BTD of EEG data for $L_r = 4, r = 1, \ldots, R$. B. Fit versus rank number L_r obtained by computing the BTD of EEG data for $R = 5$.

node factor matrix with rank-L_r, which is able to characterize the topological structures of the latent network pattern. That is the rank-L_r encodes L_r communities or node clusters. Actually, tensor decomposition with the CP model can be considered a special case of rank-$(L_r, L_r, 1)$ block term decomposition (i.e., $L_r = 1$). Intuitively, the rank L_r of the node factor matrix is capable of characterizing the membership of nodes in the network. This, on the other hand, explains why the tensor decomposition with the CP model fails to detect the community structures ($L_r = 1$ one community left).

The key parameters for the BTD-based methods are the determination of the component number and rank number, which is less well prescribed and not a limitation of the proposed approach directly. In the absence of theoretically motivated methods for parameter selection, we here opted instead to repeat the data fitting analysis for different values to select a relatively rational number. Fig. 4A shows the data fitting with different component numbers when fixing the rank $L_r = 4$. We can see the data fitting no longer increases or increases slowly when $R = 5$. Fig. 4B shows the data fitting with different rank numbers, indicating that data fitting almost stays constant as L_r increases. Finally, we set the $R = 5$ and $L_r = 4$ according to the data fitting analysis and previous experience. Note that such data fitting analysis only provides a reference and instruction and is not able to accurately estimate the underlying true numbers of BTD components.

For the parcellation, we chose the DK atlas as the template since the scalp electrodes are not very dense. Although beyond the scope of the current work, the other atlas could also be used in our method after source leakage correction. In addition, note that the topological structure with specific four modules is a whole pattern with one corresponding temporal evolution instead of four independent module patterns.

V. Conclusion

We introduced a framework based on a latent network generative model and related it to BTD for detecting dynamic community evolution in time-varying brain networks during continuous music listening. It allows us to identify the topological structures of dynamic brain networks and their time evolution during naturalistic stimuli. The majority of approaches for brain networks failed to reveal the topological structures of time-varying networks. Here, we apply block component analysis, rank-$(L_r, L_r, 1)$ BTD, to the adjacent tensor. The node factor matrix of BTD components with rank-L_r is able to characterize the topological structures of the latent network pattern, which encodes L_r communities or node clusters. We validate the proposed method in simulation and then apply it to the EEG data recorded during free music listening. The identified brain patterns with distinct topological structures were in line with those previously published in the fMRI and EEG studies. The proposed method looks valuable for the characterization of the temporal evolution of brain networks with specific community structures during freely listening to music or other naturalistic stimuli.

References

[1] E. Bullmore and O. Sporns, "Complex brain networks: Graph theoretical analysis of structural and functional systems," *Nature Rev. Neurosci.*, vol. 10, no. 3, pp. 186–198, Mar. 2009.

[2] K. J. Friston, "Functional and effective connectivity in neuroimaging: A synthesis," *Hum. Brain Mapping*, vol. 2, nos. 1–2, pp. 56–78, 1994.

[3] F. De Pasquale et al., "Temporal dynamics of spontaneous meg activity in brain networks," *Proc. Nat. Acad. Sci. USA*, vol. 107, no. 13, pp. 6040–6045, 2010.

[4] M. J. Brookes et al., "Investigating the electrophysiological basis of resting state networks using magnetoencephalography," *Proc. Nat. Acad. Sci. USA*, vol. 108, no. 40, pp. 16783–16788, Oct. 2011.

[5] B. He et al., "Electrophysiological brain connectivity: Theory and implementation," *IEEE Trans. Biomed. Eng.*, vol. 66, no. 7, pp. 2115–2137, Jul. 2019.

[6] R. M. Hutchison et al., "Dynamic functional connectivity: Promise, issues, and interpretations," *NeuroImage*, vol. 80, pp. 360–378, Oct. 2013.

[7] D. Vidaurre et al., "Discovering dynamic brain networks from big data in rest and task," *NeuroImage*, vol. 180, pp. 646–656, Oct. 2018.

[8] A. Kabbara et al., "Detecting modular brain states in rest and task," *Netw. Neurosci.*, vol. 3, no. 3, pp. 878–901, Jan. 2019.

[9] Y. Zhu, J. Liu, K. Mathiak, T. Ristaniemi, and F. Cong, "Deriving electrophysiological brain network connectivity via tensor component analysis during freely listening to music," *IEEE Trans. Neural Syst. Rehabil. Eng.*, vol. 28, no. 2, pp. 409–418, Feb. 2020.

[10] Y. Zhu, J. Liu, T. Ristaniemi, and F. Cong, "Distinct patterns of functional connectivity during the comprehension of natural, narrative speech," *Int. J. Neural Syst.*, vol. 30, no. 3, Mar. 2020, Art. no. 2050007.

[11] C. J. Stam, "Modern network science of neurological disorders," *Nature Rev. Neurosci.*, vol. 15, no. 10, pp. 683–695, Oct. 2014.

[12] U. Braun, A. Schaefer, R. F. Betzel, H. Tost, A. Meyer-Lindenberg, and D. S. Bassett, "From maps to multi-dimensional network mechanisms of mental disorders," *Neuron*, vol. 97, no. 1, pp. 14–31, Jan. 2018.

[13] Y. Zhu et al., "Altered EEG oscillatory brain networks during music-listening in major depression," *Int. J. Neural Syst.*, vol. 31, no. 3, Mar. 2021, Art. no. 2150001.

[14] E. A. Allen, E. Damaraju, S. M. Plis, E. B. Erhardt, T. Eichele, and V. D. Calhoun, "Tracking whole-brain connectivity dynamics in the resting state," *Cerebral Cortex*, vol. 24, no. 3, pp. 663–676, Mar. 2014.

[15] A. P. Baker et al., "Fast transient networks in spontaneous human brain activity," *eLife*, vol. 3, Mar. 2014, Art. no. e01867.

[16] D. Vidaurre, S. M. Smith, and M. W. Woolrich, "Brain network dynamics are hierarchically organized in time," *Proc. Nat. Acad. Sci. USA*, vol. 114, no. 48, pp. 12827–12832, Nov. 2017.

[17] G. C. O'Neill, P. Tewarie, D. Vidaurre, L. Liuzzi, M. W. Woolrich, and M. J. Brookes, "Dynamics of large-scale electrophysiological networks: A technical review," *NeuroImage*, vol. 180, pp. 559–576, Oct. 2018.

[18] C. Ting, S. B. Samdin, M. Tang, and H. Ombao, "Detecting dynamic community structure in functional brain networks across individuals: A multilayer approach," *IEEE Trans. Med. Imag.*, vol. 40, no. 2, pp. 468–480, Feb. 2021.

[19] R. F. Betzel, L. Byrge, Y. He, J. Goñi, X.-N. Zuo, and O. Sporns, "Changes in structural and functional connectivity among resting-state networks across the human lifespan," *NeuroImage*, vol. 102, pp. 345–357, Nov. 2014.

[20] O. Sporns and R. F. Betzel, "Modular brain networks," *Annu. Rev. Psychol.*, vol. 67, no. 1, pp. 613–640, Jan. 2016.

[21] L. E. Suárez, R. D. Markello, R. F. Betzel, and B. Misic, "Linking structure and function in macroscale brain networks," *Trends Cogn. Sci.*, vol. 24, no. 4, pp. 302–315, Apr. 2020.

[22] M. E. J. Newman and M. Girvan, "Finding and evaluating community structure in networks," *Phys. Rev. E, Stat. Phys. Plasmas Fluids Relat. Interdiscip. Top.*, vol. 69, no. 2, Feb. 2004, Art. no. 026113.

[23] D. S. Bassett, N. F. Wymbs, M. A. Porter, P. J. Mucha, J. M. Carlson, and S. T. Grafton, "Dynamic reconfiguration of human brain networks during learning," *Proc. Nat. Acad. Sci. USA*, vol. 108, no. 18, pp. 7641–7646, May 2011.

[24] J. Ou et al., "Characterizing and differentiating brain state dynamics via hidden Markov models," *Brain Topogr.*, vol. 28, no. 5, pp. 666–679, Sep. 2015.

[25] S. Ma, V. D. Calhoun, R. Phlypo, and T. Adalı, "Dynamic changes of spatial functional network connectivity in healthy individuals and schizophrenia patients using independent vector analysis," *NeuroImage*, vol. 90, pp. 196–206, Apr. 2014.

[26] D. Vidaurre, A. J. Quinn, A. P. Baker, D. Dupret, A. Tejero-Cantero, and M. W. Woolrich, "Spectrally resolved fast transient brain states in electrophysiological data," *NeuroImage*, vol. 126, pp. 81–95, Feb. 2016.

[27] D. Vidaurre et al., "Spontaneous cortical activity transiently organises into frequency specific phase-coupling networks," *Nature Commun.*, vol. 9, no. 1, pp. 1–13, Jul. 2018.

[28] N. Leonardi et al., "Principal components of functional connectivity: A new approach to study dynamic brain connectivity during rest," *NeuroImage*, vol. 83, pp. 937–950, Dec. 2013.

[29] G. C. O'Neill et al., "Measurement of dynamic task related functional networks using MEG," *NeuroImage*, vol. 146, pp. 667–678, Feb. 2017.

[30] P. J. Mucha, T. Richardson, K. Macon, M. A. Porter, and J.-P. Onnela, "Community structure in time-dependent, multiscale, and multiplex networks," *Science*, vol. 328, no. 5980, pp. 876–878, May 2010.

[31] E. Al-Sharoa, M. Al-Khassaweneh, and S. Aviyente, "Tensor based temporal and multilayer community detection for studying brain dynamics during resting state fMRI," *IEEE Trans. Biomed. Eng.*, vol. 66, no. 3, pp. 695–709, Mar. 2019.

[32] L.-E. Martinet et al., "Robust dynamic community detection with applications to human brain functional networks," *Nature Commun.*, vol. 11, no. 1, pp. 1–13, Jun. 2020.

[33] J. M. Mueller et al., "Dynamic community detection reveals transient reorganization of functional brain networks across a female menstrual cycle," *Netw. Neurosci.*, vol. 5, no. 1, pp. 125–144, Jan. 2021.

[34] K. Tu, B. Ribeiro, A. Swami, and D. Towsley, "Temporal clustering in dynamic networks with tensor decomposition," 2016, *arXiv:1605.08074*.

[35] Z. Chen, C. Chen, Z. Zheng, and Y. Zhu, "Tensor decomposition for multilayer networks clustering," in *Proc. AAAI Conf. Artif. Intell.*, vol. 33, 2019, pp. 3371–3378.

[36] E. Al-sharoa, M. A. Al-khassaweneh, and S. Aviyente, "Detecting and tracking community structure in temporal networks: A low-rank + sparse estimation based evolutionary clustering approach," *IEEE Trans. Signal Inf. Process. Netw.*, vol. 5, no. 4, pp. 723–738, Dec. 2019.

[37] G. Frusque, J. Jung, P. Borgnat, and P. Gonçalves, "Multiplex network inference with sparse tensor decomposition for functional connectivity," *IEEE Trans. Signal Inf. Process. Netw.*, vol. 6, pp. 316–328, 2020.

[38] Y. Zhu, X. Li, T. Ristaniemi, and F. Cong, "Measuring the task induced oscillatory brain activity using tensor decomposition," in *Proc. IEEE Int. Conf. Acoust., Speech Signal Process. (ICASSP)*, May 2019, pp. 8593–8597.

[39] Y. Zhu et al., "Discovering dynamic task-modulated functional networks with specific spectral modes using MEG," *NeuroImage*, vol. 218, Sep. 2020, Art. no. 116924.

[40] J. Liu, Y. Zhu, H. Sun, T. Ristaniemi, and F. Cong, "Sustaining attention for a prolonged duration affects dynamic organizations of frequency-specific functional connectivity," *Brain Topogr.*, vol. 33, no. 6, pp. 677–692, Nov. 2020.

[41] E. Acar, M. Roald, K. M. Hossain, V. D. Calhoun, and T. Adali, "Tracing evolving networks using tensor factorizations vs. ICA-based approaches," *Frontiers Neurosci.*, vol. 16, Apr. 2022, Art. no. 861402.

[42] M. Roald, S. Bhinge, C. Jia, V. Calhoun, T. Adalı, and E. Acar, "Tracing network evolution using the Parafac2 model," in *Proc. IEEE Int. Conf. Acoust., Speech Signal Process. (ICASSP)*, May 2020, pp. 1100–1104.

[43] L. Gauvin, A. Panisson, and C. Cattuto, "Detecting the community structure and activity patterns of temporal networks: A non-negative tensor factorization approach," *PLoS ONE*, vol. 9, no. 1, Jan. 2014, Art. no. e86028.

[44] L. De Lathauwer, "Decompositions of a higher-order tensor in block terms—Part II: Definitions and uniqueness," *SIAM J. Matrix Anal. Appl.*, vol. 30, no. 3, pp. 1033–1066, Jan. 2008.

[45] G. Zhou, A. Cichocki, Q. Zhao, and S. Xie, "Nonnegative matrix and tensor factorizations: An algorithmic perspective," *IEEE Signal Process. Mag.*, vol. 31, no. 3, pp. 54–65, May 2014.

[46] A. Cichocki et al., "Tensor decompositions for signal processing applications: From two-way to multiway component analysis," *IEEE Signal Process. Mag.*, vol. 32, no. 2, pp. 145–163, Mar. 2015.

[47] N. D. Sidiropoulos, L. De Lathauwer, X. Fu, K. Huang, E. E. Papalexakis, and C. Faloutsos, "Tensor decomposition for signal processing and machine learning," *IEEE Trans. Signal Process.*, vol. 65, no. 13, pp. 3551–3582, Jul. 2017.

[48] F. Cong et al., "Linking brain responses to naturalistic music through analysis of ongoing EEG and stimulus features," *IEEE Trans. Multimedia*, vol. 15, no. 5, pp. 1060–1069, Aug. 2013.

[49] L. De Lathauwer and D. Nion, "Decompositions of a higher-order tensor in block terms—Part III: Alternating least squares algorithms," *SIAM J. Matrix Anal. Appl.*, vol. 30, no. 3, pp. 1067–1083, Jan. 2008.

[50] V. Alluri, P. Toiviainen, I. P. Jääskeläinen, E. Glerean, M. Sams, and E. Brattico, "Large-scale brain networks emerge from dynamic processing of musical timbre, key and rhythm," *NeuroImage*, vol. 59, no. 4, pp. 3677–3689, Feb. 2012.

[51] Y. Zhu et al., "Exploring frequency-dependent brain networks from ongoing EEG using spatial ICA during music listening," *Brain Topogr.*, vol. 33, no. 3, pp. 289–302, May 2020.

[52] A. Hyvärinen and E. Oja, "Independent component analysis: Algorithms and applications," *Neural Netw.*, vol. 13, nos. 4–5, pp. 411–430, Jun. 2000.

[53] F. Tadel, S. Baillet, J. C. Mosher, D. Pantazis, and R. M. Leahy, "Brainstorm: A user-friendly application for MEG/EEG analysis," *Comput. Intell. Neurosci.*, vol. 2011, pp. 1–13, Jan. 2011.

[54] F.-H. Lin, J. W. Belliveau, A. M. Dale, and M. S. Hämäläinen, "Distributed current estimates using cortical orientation constraints," *Hum. Brain Mapping*, vol. 27, no. 1, pp. 1–13, Jan. 2006.

[55] R. S. Desikan et al., "An automated labeling system for subdividing the human cerebral cortex on MRI scans into gyral based regions of interest," *NeuroImage*, vol. 31, no. 3, pp. 968–980, Jul. 2006.

[56] J. F. Hipp, D. J. Hawellek, M. Corbetta, M. Siegel, and A. K. Engel, "Large-scale cortical correlation structure of spontaneous oscillatory activity," *Nature Neurosci.*, vol. 15, no. 6, pp. 884–890, Jun. 2012.

[57] A. Cichocki, R. Zdunek, A. H. Phan, and S.-I. Amari, *Nonnegative Matrix and Tensor Factorizations: Applications to Exploratory Multiway Data Analysis and Blind Source Separation*. Hoboken, NJ, USA: Wiley, 2009.

[58] N. Vervliet, O. Debals, L. Sorber, M. Van Barel, and L. De Lathauwer, "Tensorlab 3.0," Mar. 2016. [Online]. Available: https://www.tensorlab.net

[59] Y. Cheng, M. Riesmeyer, J. Haueisen, and M. Haardt, "Using the multi-linear rank-$(L_r, L_r, 1)$ decomposition for the detection of the 200 Hz band activity in somatosensory evoked magnetic fields and somatosensory evoked electrical potentials," *IEEE Access*, vol. 9, pp. 106232–106244, 2021.

[60] D. Prichard and J. Theiler, "Generating surrogate data for time series with several simultaneously measured variables," *Phys. Rev. Lett.*, vol. 73, no. 7, pp. 951–954, Aug. 1994.

[61] L. Fadiga, L. Craighero, and A. D'Ausilio, "Broca's area in language, action, and music," *Ann. New York Acad. Sci.*, vol. 1169, no. 1, pp. 448–458, Jul. 2009.

[62] S. Koelsch, E. Kasper, D. Sammler, K. Schulze, T. Gunter, and A. D. Friederici, "Music, language and meaning: Brain signatures of semantic processing," *Nature Neurosci.*, vol. 7, no. 3, pp. 302–307, Mar. 2004.

[63] V. Alluri, P. Toiviainen, I. Burunat, M. Kliuchko, P. Vuust, and E. Brattico, "Connectivity patterns during music listening: Evidence for action-based processing in musicians," *Hum. Brain Mapping*, vol. 38, no. 6, pp. 2955–2970, Jun. 2017.